Phosphorylation on PstP controls cell wall metabolism and antibiotic tolerance in *Mycobacterium smegmatis*

Farah Shamma[1], Kadamba Papavinasasundaram[2], Aditya Bandekar[2], Christopher Sassetti[2], and Cara C. Boutte[1]*

[1]Department of Biology, University of Texas Arlington, Arlington, Texas

[2]Department of Microbiology and Physiological Systems, University of Massachusetts Medical School, Worcester, Massachusetts

*corresponding author: cara.boutte@uta.edu

Running title: Phosphorylation of PstP affects the cell wall

Key words:

PstP, Serine/Threonine Phosphatase, peptidoglycan metabolism, mycolic acid metabolism, antibiotic tolerance, Mycobacteria, cell wall metabolism, CwlM, dephosphorylation

Abstract

Mycobacterium tuberculosis and its relatives have dynamic cell walls that respond to environmental stresses. Modulation of cell wall metabolism under stress is thought to be responsible for decreased cell wall permeability and increased tolerance to antibiotics. The signaling pathways that control cell wall metabolism under stress, however, are poorly understood. Here, we examine the signaling capacity of a cell wall master regulator, the Serine Threonine Phosphatase PstP, in the model organism *Mycobacterium smegmatis.* We studied how interference with a regulatory phosphorylation site on PstP affects growth, cell wall metabolism and antibiotic tolerance. We find that a phospho-mimetic mutation, *pstP* T171E, slows growth, misregulates both mycolic acid and peptidoglycan metabolism in different conditions, and interferes with antibiotic tolerance. We show that the peptidoglycan regulator CwlM is a substrate of PstP, and may be an important mediator of PstP's role in controlling peptidoglycan metabolism. These data suggest that phosphorylation on PstP affects its activity and is important in the transition between growth and stasis.

Importance

Regulation of cell wall assembly is essential for bacterial survival and contributes to pathogenesis and antibiotic tolerance in mycobacteria, including pathogens such as *Mycobacterium tuberculosis*. However, little is known about how the cell wall is regulated in stress. We describe a mechanism of cell wall modulation

47 in *Mycobacterium smegmatis* through the only essential Ser/Thr phosphatase
48 PstP. We showed that phosphorylation on PstP regulates peptidoglycan
49 metabolism in the transition to stasis and the mycolic acid metabolism in growth.
50 This regulation also affects antibiotic tolerance. This work helps us to understand
51 the phosphorylation/dephosphorylation-mediated cell wall regulation circuitry in
52 Mycobacteria. We propose PstP to be a cell wall master regulator that can be a
53 potential drug target.
54
55 **Introduction**
56
57 Tuberculosis (TB), an infectious disease caused by the bacterium
58 *Mycobacterium tuberculosis* (*Mtb*) is one of the leading infectious causes of
59 death (1). The fact that TB treatment requires at least a six month regimen with
60 four antibiotics is partly due to the intrinsic phenotypic antibiotic tolerance of *Mtb*
61 (2, 3). Stressed *Mtb* cells can achieve a dormant, non-replicating state exhibiting
62 antibiotic tolerance, cell wall thickening and altered cell-wall staining (4-7). The
63 changes in the cell wall and reduced permeability to antibiotics in stressed cells
64 (8) suggest that the regulation of the cell wall is a major contributor to antibiotic
65 tolerance.
66
67 The accepted cell wall core architecture of *Mtb* consists of a single mycolyl-
68 arabinogalactan-peptidoglycan molecule which is composed of three covalently
69 linked layers (9). A peptidoglycan (PG) layer surrounding the plasma membrane

70 is covalently bound to an arabinogalactan layer. A lipid layer composed of
71 mycolic acids surrounds the arabinogalactan layer, and the inner leaflet of this
72 layer is covalently linked to the arabinogalactan (10). The outer leaflet of the
73 mycolic acid layer contains free mycolic acids, trehalose mycolates and other
74 lipids, glycolipids, glycans and proteins (11). The mycolic acid layer is the major
75 contributor to impermeability of the cell wall (12-14).
76
77 While much is known about the cell wall structure of *Mtb*, little is known about its
78 regulation during stress, or how this contributes to antibiotic tolerance. The
79 signaling pathways regulating the *Mtb* cell wall likely help it survive in the host.
80 Reversible protein phosphorylation is a key regulatory tool used by bacteria for
81 environmental signal transduction to regulate cell growth (15-18). In *Mtb*,
82 Serine/Threonine phosphorylation is important in cell wall regulation (19). *Mtb*
83 has 11 Serine/Threonine Protein Kinases (STPKs) (PknA, PknB and PknD-L)
84 and only one Serine/Threonine protein phosphatase (PstP) (20, 21).
85
86 Among the STPKs, PknA and PknB are essential for *Mtb* growth and
87 phosphorylate substrates involved in cell growth and division (22-26). Some of
88 these substrates are enzymes whose activity is directly altered by
89 phosphorylation. For example, all the enzymes in the FAS-II system of mycolic
90 acid biosynthesis are regulated by threonine phosphorylation (27-33).
91
92 There are also cell wall regulators that are not enzymes but whose

93 phosphorylation by STPKs affects cell shape and growth. For example, the
94 regulator CwlM activates MurA (26), the first enzyme in PG precursor
95 biosynthesis (34), when it is phosphorylated by PknB. In the transition to
96 starvation, CwlM is rapidly dephosphorylated in *Mycobacterium smegmatis*
97 (*Msmeg)* (26). Misregulation of MurA activity increases sensitivity to antibiotics in
98 early starvation (26), implying that phospho-regulation of CwlM promotes
99 antibiotic tolerance. CwlM may also regulate other steps of PG synthesis (35). A
100 recent phosphoproteomic study showed that transcriptional repression of the
101 operon that contains both *pstP* and *pknB* leads to increased phosphorylation of
102 CwlM (36). While the effects of the individual genes were not separated (36), this
103 suggests that PstP could dephosphorylate CwlM.
104
105 PstP is essential in *Mtb* and *Msmeg* (37, 38). It is a member of the Protein
106 phosphatase 2C (PP2C) subfamily of metal-dependent protein Serine/Threonine
107 phosphatases (39) which strictly require divalent metal ions for activity (40), (41).
108 PP2C phosphatases are involved in responding to environmental signals,
109 regulating metabolic processes, sporulation, cell growth, division and stress
110 response in a diverse range of prokaryotes and eukaryotes (42-47).
111
112 $PstP_{Mtb}$ shares structural folds and conserved residues with the human PP2Cα
113 (48), which serves as the representative of the PP2C family. $PstP_{Mtb}$ has an N-
114 terminal cytoplasmic enzymatic domain, a transmembrane pass and a C-terminal
115 extracellular domain (39) (Fig. 1A).

116 Many of the proteins known to be dephosphorylated by PstP (27, 39, 49-52) are
117 involved in cell wall metabolism; however, the effects of this activity differ. For
118 example, dephosphorylation of CwlM should decrease PG metabolism (26). But
119 dephosphorylation of all the FAS-II enzymes (27-32) should upregulate lipid
120 metabolism. As PG and lipid metabolism should be coordinated (53), PstP must
121 be able to minutely choose its substrates in growth and stasis. For example, we
122 expect that PstP should dephosphorylate KasA but not CwlM during growth, and
123 should switch this specificity in stasis.
124
125 $PstP_{Mtb}$ is itself phosphorylated on Threonine residues 137, 141, 174 and 290
126 (49). We hypothesize that phosphorylation of the threonine residues of PstP
127 might help coordinate activity against different substrates through changes in
128 access to substrates or binding affinity to substrates or regulators.
129
130 We report here that phospho-ablative and phospho-mimetic mutations at the
131 phospho-site T171 of $PstP_{Msmeg}$ alter growth rate, cell length, cell wall metabolism
132 and antibiotic tolerance. Strains of *Msmeg* with *pstP* T171E alleles grow slowly,
133 are unable to properly downregulate PG metabolism and upregulate antibiotic
134 tolerance in the transition to starvation. We observed that the same mutation has
135 nearly opposite effects on mycolic acid layer metabolism. We also report that
136 $PstP_{Mtb}$ dephosphorylates $CwlM_{Mtb.}$
137
138

139 **Materials and Methods**

140

141 **Bacterial strains and culture conditions**

142

143 All *Mycobacterium smegmatis* mc^{2}155 ATCC 700084 cultures were started in
144 7H9 (Becton, Dickinson, Franklin Lakes, NJ) medium containing 5 g/liter bovine
145 serum albumin (BSA), 2 g/liter dextrose, 0.003 g/liter catalase, 0.85 g/liter NaCl,
146 0.2% glycerol, and 0.05% Tween 80 and incubated at 37°C up to log. phase.
147 Hartmans-de Bont (HdB) minimal medium made as described previously (54)
148 without glycerol was used for starvation assays. Serial dilutions of all CFU counts
149 were plated on on LB Lennox agar (Fisher BP1427-2).

150

151 *E. coli* Top10, XL1Blue and Dh5α were used for cloning and *E. coli* BL21 Codon
152 Plus was used for protein expression. Antibiotic concentrations for *M. smegmatis*
153 were 25 µg/ml kanamycin. 50 µg/ml hygromycin and 20 µg/ml zeocin. Antibiotic
154 concentrations for *E. coli* were 50 µg/ml kanamycin, 25 µg/ml zeocin, 20 µg/ml
155 chloramphenicol and 140 µg/ml ampicillin.

156

157 **Strain construction**

158

159 The PstP$_{Msmeg}$-knockdown strain was made first by creating a merodiploid strain
160 and then by deleting the native *pstP*$_{Msmeg}$ gene from its chromosomal location.
161 The merodiploid strain was generated by introducing a constitutively expressing

162 *pstP*$_{Mtb}$ gene cloned on an StrR plasmid at the L5 attB integration site. The
163 *pstP*$_{Msmeg}$ gene (MSMEG_0033) at the native locus was then deleted by RecET-
164 mediated double stranded recombineering approach using a 1.53 kb loxP-hyg-
165 loxP fragment carrying a 125 bp DNA flanking the *pstP*$_{Msmeg}$ gene, as described
166 (55). The recombineering substrate was generated by two sequential overlapping
167 PCR of the loxP-hyg-loxP substrate present in the plasmid pKM342. The
168 downstream flanking primer used in the first PCR also carried an optimized
169 mycobacterial ribosome binding site in front of the start codon of MSMEG_0032
170 to facilitate the expression of the genes present downstream of *pstP*$_{Msmeg}$ *in* the
171 *Msmeg pstP-pknB* operon.
172
173 Deletion of the *pstP*$_{Msme}$ gene was confirmed by PCR amplification and
174 sequencing of the 5' and 3' recombinant junctions, and the absence of an internal
175 wild-type *pstP*$_{Msmeg}$ PCR product. The *pstP*$_{Mtb}$ allele present at the L5 site was
176 then swapped, as described (56), with a tet-regulatable *pstP*$_{Mtb}$ allele (RevTetR-
177 P750- *pstP*$_{Mtb}$-DAS tag-L5-Zeo plasmid). The loxP-flanked *hyg* marker present in
178 the chromosomal locus was then removed by expressing Cre from pCre-sacB-
179 Kan, and the Cre plasmid was subsequently cured from this strain by plating on
180 sucrose. We named this strain CB1175.
181
182 Different alleles of *pstP* were attained by swapping the Wild-type (WT) allele at
183 L5 site of CB1175 as described (57). In order to do so, the wild-type (WT) and
184 the phosphoablative alleles of *pstP*$_{Msmeg}$ alleles were at first cloned individually

185 into a kanamycin resistant-marked L5 vector pCT94 under a TetO promoter to
186 generate vectors pCB1206-1208 and pCB1210, which would swap out the
187 zeocin-resistance marked vector at the L5 site in CB1175. The pTetO was a
188 strong promoter and we were having trouble getting transformants when CB1175
189 was transformed with these vectors.
190
191 So, the TetO promoter was excised from each these constructs and an
192 intermediate strength promoter p766TetON6 was cloned from the vector
193 pCB1030 (pGMCgS-TetON-6 sspB) into each of the vectors pCB1206-1208 and
194 pCB1210 to generate the L5 vectors pCB1282-85 now containing various *pstP*
195 alleles under p766tetON6. pCB1285 was used as the parent vector to clone in
196 the phosphomimetic *pstP* alleles under p766TetON6.
197
198 These kanamycin resistance-marked vector constructs were then used to swap
199 out the zeocin resistance-marked vector at the L5 site of CB1175 to attain
200 different allelic strains of *pstP* as described (57).
201
202 **Growth Curve assay**
203
204 Biological triplicates of each strain were grown in 7H9 media up to log. phase.
205 Growth curve experiment was performed in non-treated 96 well plate using plate
206 reader (BioTek Synergy neo2 multi mode reader) in 200ul 7H9 media starting at

207 OD_{600}=0.1 for 16 hours at 37°C. Data was analyzed using the software Prism
208 (version 7.0d).
209
210 **Cell staining**
211
212 For staining cells in log. phase, 100 µl culture in 7H9 was incubated at 37°C with
213 1ul of 10mM DMN-Tre for 30 minutes and 1µl of 10mM HADA for 15 minutes.
214 Cells were then pelleted and resuspended in 1x phosphate buffered saline (PBS)
215 supplemented with 0.05% Tween 80 and fixed with 10µl of 16%
216 parafolmaldehyde (PFA) for 10 minutes at room temperature. After spinning
217 down, cells were finally resuspended in PBS + Tween 80.
218
219 For starvation microscopy, cultures were shaken for 4 hours in HdB media
220 without glycerol at 37°C. 500µl of each culture were pelleted and concentrated to
221 100µl, then incubated at 37°C with 1µl of 10mM DMN-Tre for 1 hour and 3µl of
222 10mM HADA for 30 minutes. Cells were then washed and fixed as above. The
223 total time of starvation before fixation was 5.5 hours.
224
225 **Microscopy and Image Analysis**
226
227 Cells were imaged with a Nikon Ti-2 widefield epifluorescence microscope with a
228 Photometrics Prime 95B camera and a Plan Apo 100x, 1.45 numerical aperture
229 objective lens. The green fluorescence images for DMN-Tre staining were taken

230 with a 470/40nm excitation filter and a 525/50nm emission filter. Blue
231 fluorescence images for HADA staining were taken using 350/50nm excitation
232 filter and 460/50nm emission filter. All images were captured using NIS Elements
233 software and analyzed using FIJI and MicrobeJ (58)
234
235
236 **Western Blots**
237
238 Cultures were grown in 7H9 to OD_{600}=0.8 in 10ml 7H9 media, pelleted and
239 resuspended in 500µL PBS with 1mM PMSF and lysed (MiniBeadBeater-16,
240 Model 607, Biospec). Supernatants from the cell lysate were run on 12%
241 resolving Tris-Glycine gels and then transferred onto PVDF membrane (GE
242 Healthcare). Rabbit α-strep antibody (1:1000, Abcam, ab76949) in TBST buffer
243 with 0.5% milk and goat α-rabbit IgG (H+L) HRP conjugated secondary antibody
244 (1:10,000, ThermoFisher Scientific 31460) in TBST were used to detect PstP-
245 strep. For starvation experiments, cultures were first grown to log. phase, then
246 starved in HdB no glycerol media staring at OD=0.5 for 1.5 hour.
247
248 For Western blots of *in vitro* assays, samples were run on 12% SDS gel (Mini-
249 Protean TGX, Biorad, 4561046) and then transferred onto PVDF membrane (GE
250 Healthcare). Mouse α-His antibody (1:1000, Genscript A00186) in TBST buffer
251 with 0.5% BSA and goat α-mouse IgG (H+L) HRP conjugated secondary
252 antibody (1:10,000, Invitrogen A28177) were used to detect His-tagged proteins

253 on the blot. The blot was stripped off using stripping buffer (Thermo Scientific,
254 21059) and re-probed with Rabbit α-Phospho-Threonine antibody (1:1000, Cell
255 Signaling #9381) and goat α-rabbit IgG (H+L) HRP conjugated secondary
256 antibody (1:10,000, ThermoFisher Scientific 31460) to detect phosphorylation on
257 the blot.
258
259 **Antibiotic assays**
260
261 For antibiotic assays in log. phase, log. phase cultures were diluted in 7H9 media
262 to OD600= 0.05 before treatment. For starvation assays, cells were grown to
263 OD_{600}=0.5, pelleted, washed and resuspended in HdB starvation (with no
264 glycerol and 0.05% Tween) media at OD_{600}=0.3 and incubated at 37°C for a total
265 of five a half hours. The cultures were then diluted to OD_{600}=0.05 before antibiotic
266 treatment. 8 µg/ml and 45 µg/ml Meropenem was used for log. phase and
267 starved cultures, respectively. 10 µg/ml and 90 ug/ml Isoniazid was added to log-
268 phase and starved cultures, respectively. Samples from the culture were serially
269 diluted and plated on LB agar before and after treatment, and colony forming
270 units were calculated.
271
272 **Protein Purification**
273
274 All the proteins were expressed using *E. coli* BL 21 Codon Plus cells.

275 N-terminally his-MBP tagged $PknB_{Mtb}$ was expressed and purified as described
276 (59). His-$PstP_cWT_{Mtb}$ (1-300 amino acids of the cytosolic domain, (60)) and His-
277 SUMO-$CwlM_{Mtb}$ were both expressed overnight by IPTG induction, purified on Ni-
278 NTA resin (G-Biosciences, #786-940 in 5 ml Bio-Scale™ Mini Cartridges, BioRad
279 #7324661), then dialyzed, concentrated and run over size exclusion resin (GE
280 Biosciences Sephacryl S-200 in HiPrep 26/70 column) to obtain soluble proteins.
281 The buffer for His-SUMO-$CwlM_{Mtb}$ was 50mM Tris pH 8, 350mM NaCl, 1mM DTT
282 and 10% glycerol. The buffer for His-$PstP_cWT_{Mtb}$ was 50mM Tris pH 7.5, 350mM
283 NaCl, 1mM DTT and 10% glycerol. 20mM imidazole was added to each buffer for
284 lysis and application to the Ni-NTA column, and 250mM imidazole was added for
285 elution. His-$PstP_cT174E_{Mtb}$ was expressed and purified using the same conditions
286 and buffers used for His-$PstP_cWT_{Mtb}$.
287
288 ***In vitro* Dephosphorylation assay**
289
290 Purified His-SUMO-$CwlM_{Mtb}$ was phosphorylated with the purified kinase His-
291 MBP-$PknB_{Mtb}$ for 1 hour at room temperature in presence of 0.5mM ATP, 1mM
292 $MnCl_2$ and buffer (50mM Tris pH 7.5, 250mM NaCl, and 1mM DTT). The amount
293 of kinase was one-tenth of the amount of substrate in the phosphorylation
294 reaction. To stop the kinase reaction by depleting ATP, 0.434 units of calf
295 intestinal alkaline phosphatase (Quick CIP, NEB, MO525S) per µg of His-SUMO-
296 $CwlM_{Mtb}$ was added to the reaction mixture and incubated for 1 hour at 37°C. The
297 reaction mixture was then divided into five parts for the different phosphatase

298 samples and a control with buffer.

299 Two individually expressed and purified batches of both His-PstP$_c$WT$_{Mtb}$ and His-
300 PstP$_c$T1714E$_{Mtb}$ were used as biological replicates to perform the
301 dephosphorylation assay. The reaction was carried out at room temperature for
302 up to 90 minutes in presence of phosphatase buffer (50mM Tris pH 7.5, 10mM
303 $MnCl_2$, and 1mM DTT). The amount of phosphatase used was half the amount of
304 His-SUMO-CwlM$_{Mtb}$.

305

306 **Results**

307

308 **Phospho-site T171 of PstP$_{Msmeg}$ has an impact on growth**

309

310 PstP is necessary for cell growth in *Msmeg* (36, 37) and phosphorylation
311 increases PstP$_{Mtb}$'s activity against small molecule substrates *in vitro* (36, 37, 49).
312 We wanted to see if the phosphorylations on PstP regulate cell growth.
313 Threonines T134, T138, and T171 in PstP$_{Msmeg}$ correspond to the phospho-sites
314 on PstP$_{Mtb}$ (49) (Fig. 1A). We constructed an *Msmeg* strain with one copy of *pstP*
315 at the L5 phage integrase site using recombineering (61). We then exchanged
316 the wild-type allele for either phospho-ablative (T>A) or phospho-mimetic (T>E)
317 alleles at each of the three conserved phosphorylation sites (57, 62).

318

319 We performed growth curves with several clones of each mutant allele. We found
320 that the biological replicates of the T134A, T134E, T138A and T138E mutant

321 strains had bi-modal distributions of doubling times (Fig. 1B). T134 and T138
322 map to the flap subdomain of $PstP_{Mtb}$ (Fig. 1A). This subdomain varies greatly in
323 sequence and structure across different PP2C family members and has been
324

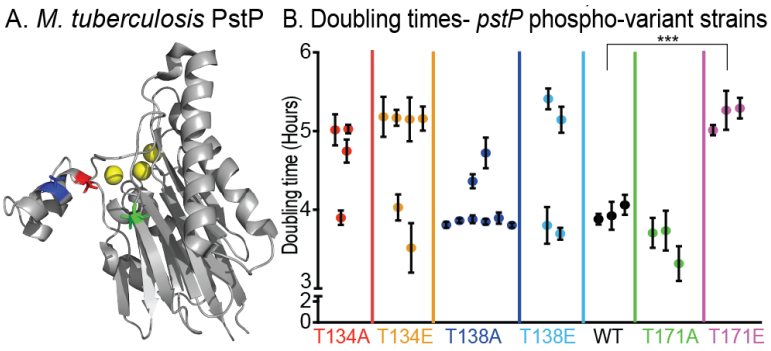

325

326 **FIG 1 Phosphosite T171 on PstP affects growth.**

327 (A) Crystal structure of PstP from *M. tuberculosis* ($PstP_{Mtb}$) (48). The threonine (T) sites on
328 $PstP_{Mtb}$ phosphorylated by the kinases PknA and PknB (49) are highlighted on the structure: red-
329 $PstP_{Mtb}$ T137 (T134 in $PstP_{Msmeg}$), blue- $PstP_{Mtb}$ T141 (T138 in $PstP_{Msmeg}$) and green- $PstP_{Mtb}$
330 T174 (T171 in $PstP_{Msmeg}$).

331 (B) Doubling times of strains containing $pstP_{Msmeg}$WT, phosphoablative mutant alleles $pstP_{Msmeg}$
332 T134A, T138A and T171A and phosphomimetic mutant alleles $pstP_{Msmeg}$ T134E, T138E and
333 T171E. Each dot is the mean of doubling times from two to three different experiments on
334 different dates of a single isolated clone. The error bars represent the standard deviation. P
335 value= 0.0009.

336

337 shown to be important in regulating substrate binding, specificity and catalytic
338 activity (48, 63-65). Particularly, T138A and T138E variants of the serine
339 threonine phosphatase tPphA from *Thermosynechococcus elongatus* showed
340 differences in substrate reactivity (63). This suggests that phosphorylation at
341 T134 and T138 could be very important in regulating the normal activity of

342 PstP$_{Msmeg}$ in the cell. We suspect that these mutations impaired growth so
343 severely that suppressor mutations formed in several of the biological replicates,
344 giving rise to the inconsistent growth rates.
345
346 The *Msmeg* strains with *pstP* T171A and T171E mutations showed consistent
347 and reproducible growth rates (Fig. 1B). The T171A mutants grew normally, but
348 the T171E grew more slowly than the wild-type. Since T171E mimics constitutive
349 phosphorylation, this result suggests that the continuous presence of a
350 phosphate on T171 inhibits cell growth.
351
352 **Phospho-site T171 of PstP$_{Msmeg}$ regulates cell length**
353 To assess how phosphorylation on T171 affects growth, we examined the cell
354 morphology of *Msmeg pstP* T171 mutants and wild-type (Fig. 2A and B).

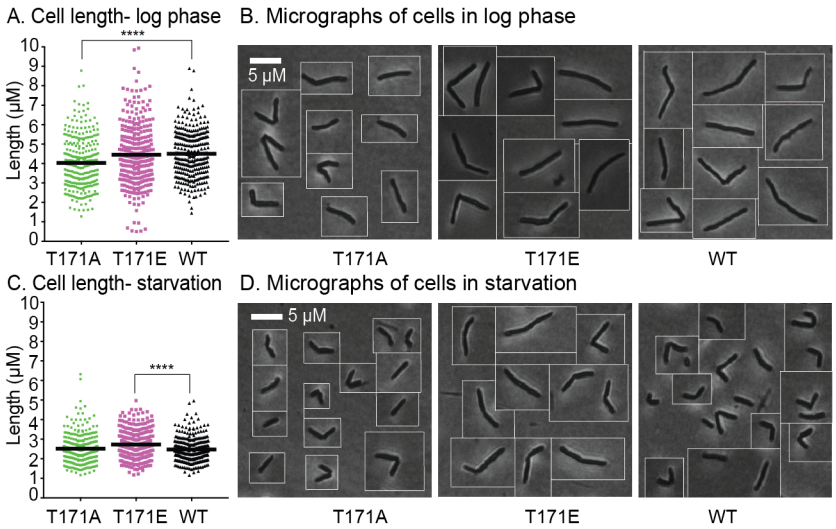

355

356 **FIG 2 Phosphosite T171 on PstP$_{Msmeg}$ is important in regulating the cell length.**

357 (A) Quantification of cell lengths of isogenic *pstP* allele strains (WT, T17A and T171E) grown in
358 7H9 in log. phase. 100 cells from each of three biological replicates were measured. P values
359 were calculated by unpaired t-test. P value = 0.000005.
360 (B) Representative phase images of cells from (A).
361 (C) Quantification of cell lengths of isogenic *pstP* allele strains (WT, T17A and T171E) after
362 starvation in HdB with no glycerol for five and a half hours. 100 cells from each of three biological
363 replicates were measured. P values were calculated by unpaired t-test. P value= 0.000003.
364 (D) Representative phase images of cells from (C).
365
366 *pstP* T171A cells were about 0.5 µm shorter than the wild-type cells, on average.
367 Because this strain grew at the same rate as wild-type (Fig.1B), we assume that
368 the rate of cell elongation is the same, but that septation may be cued at shorter
369 cell lengths. The *pstP* T171E strain has cell lengths similar to the wild-type (Fig.
370 2A and B) despite the slower growth (Fig. 1B). This suggests that
371 phosphorylation on T171 may downregulate elongation and division equally.
372
373 PstP could promote the transition from growth to stasis by downregulating the
374 activity of PknA, PknB or CwlM (26, 36, 39, 49, 52). To test if the phospho-site
375 T171 of $PstP_{Msmeg}$ affects cell length in the transition to stasis, we transferred the
376 T171 allele variant strains from log. phase to minimal HdB media with Tween 80
377 as the only source of carbon, which leads *Msmeg* cells to reductively divide (66).
378 We aerated the cultures for 5.5 hours before imaging (Fig. 2C and D). The
379 effects of phospho-mutations of $PstP_{Msmeg}$ on starved cells were the inverse of
380 what we saw in the log. phase. $pstP_{Msmeg}$ T171E cells in starvation were longer
381 than the wild-type and T171A. These data imply that phosphorylation on

382 PstP$_{Msmeg}$ T171 either slows reductive division or inhibits the downregulation of
383 cell elongation in the transition to stasis. These data suggest that
384 phosphorylation on T171 of PstP$_{Msmeg}$ may alter PstP's activity towards cell
385 growth substrates.
386
387 **Phospho-site T171 of PstP$_{Msmeg}$ regulates cell wall metabolism.**
388 Since *pstP*$_{Msmeg}$ T171 seem to play a role in regulating cell length in growth and
389 stasis, we hypothesized that it affects cell wall metabolism in different phases. To
390 test this, we used fluorescent dyes that are incorporated into either the PG or
391 mycolic acid cell wall layers and which preferentially stain metabolically active
392 cell wall (67-69). We stained T171 allele variant cells from log. phase and after
393 5.5 hours of carbon starvation with both the fluorescent D-amino acid HADA (67,
394 68) (Fig. 3A, C, D and F) and the fluorescent trehalose DMN-Tre (69) (Fig. 3B, C,
395 E and F).
396
397 The PG staining intensity between the strains was the same in log. phase (Fig.
398 3A). In starvation, the *pstP*$_{Msmeg}$ T171E mutant stained much more brightly than
399 the other strains (Fig. 3D). This suggests that phosphorylation on PstP$_{Msmeg}$ T171
400 may inhibit the downregulation of PG synthesis in the transition to stasis, but that
401 this phospho-site is not important in PG metabolism during rapid growth.
402

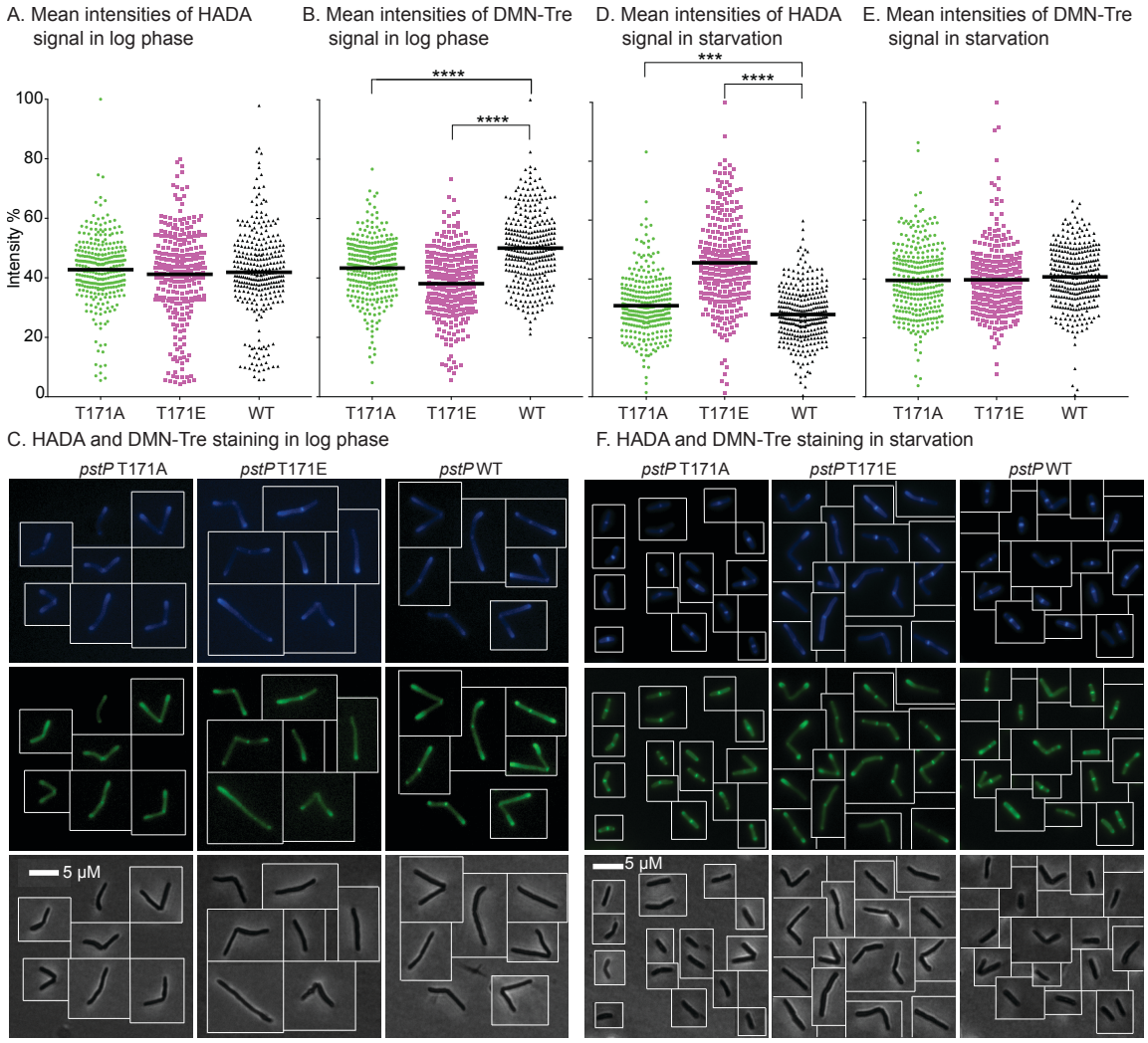

403

404 **FIG 3 Phosphosite T171 of PstP alters cell wall staining.**

405 (A) and (B) Quantification of mean intensities of HADA (A) and DMN-Tre (B) signals of *pstP* allele
406 strains (WT, T17A and T171E) in log. phase cells. Signals from 100 cells from each of three
407 biological replicates were measured using MicrobeJ. P values were calculated by unpaired t-test.
408 P values of both WT vs. T171A and WT vs. T171E= 0.000001.

409 (C) Representative micrographs of log-phase cells from (A) and (B) stained with the fluorescent
410 dyes HADA (blue) and DMN-Tre (green). Corresponding phase images are shown on the bottom
411 panel. The scale bar applies to all images.

412 (D) and (E) Quantification of mean intensities of HADA and DMN-Tre signals of starved *pstP*
413 allele strains (WT, T17A and T171E) in HdB with no glycerol. Signal from 100 cells from each of

414 three biological replicates were measured using MicrobeJ. P values were calculated by unpaired
415 t-test. P value of WT vs. T171A= 0.0002 and WT vs. T171E = 0.000001.
416 (F) Representative micrographs of starved cells from (D) stained with the fluorescent dye HADA
417 (blue) and (E) stained with the fluorescent dye DMN-Tre (green). Corresponding phase images
418 are shown on the bottom panel. The scale bar applies to all images.
419

420 Staining with DMN-Tre, which correlates with assembly of the mycolic acid cell
421 wall layer (69), shows the inverse pattern. The strains stain similarly in starvation
422 (Fig. 3E). In log. phase, however, both mutants show a significant decrease in
423 DMN-Tre signal compared to the wild-type (Fig. 3B), though the *pstP*$_{Msmeg}$ T171E
424 mutant has weaker staining that *pstP*$_{Msmeg}$ T171A. These data imply that mycolic
425 acid synthesis is regulated by phosphorylation of PstP T171 in log. phase, but
426 not in starvation. Since all the FAS-II enzymes which make mycolic acids are
427 inhibited by threonine phosphorylation (27-32), we expect that activation of PstP
428 should increase mycolic acid synthesis. These data indicate that phosphorylation
429 on PstP$_{Msmeg}$ T171 regulates mycolic acid synthesis enzymes during growth, but
430 not in starvation.
431

432 **Phospho-site T171 of PstP$_{Msmeg}$ affects antibiotic tolerance**
433

434 Stresses that arrest cell growth can cause mycobacteria to become tolerant to
435 antibiotics (8, 70-73). We hypothesized that if *Msmeg* fails to downregulate PG
436 synthesis in starvation, (Fig. 3D), then it should be more susceptible to a PG
437 targeting drug. We treated PstP$_{Msmeg}$ wild-type, T171A and T171E strains in log.

438 phase and after 5.5 hours of starvation with meropenem, and quantified survival

439 using a CFU assay. We saw that the *pstP*$_{Msmeg}$ 171E strain was more tolerant to

440 meropenem in log. phase (Fig. 4A), but more susceptible in starvation, compared

441 to *pstP*$_{Msmeg}$ T171A and wild-type strains (Fig. 4B).

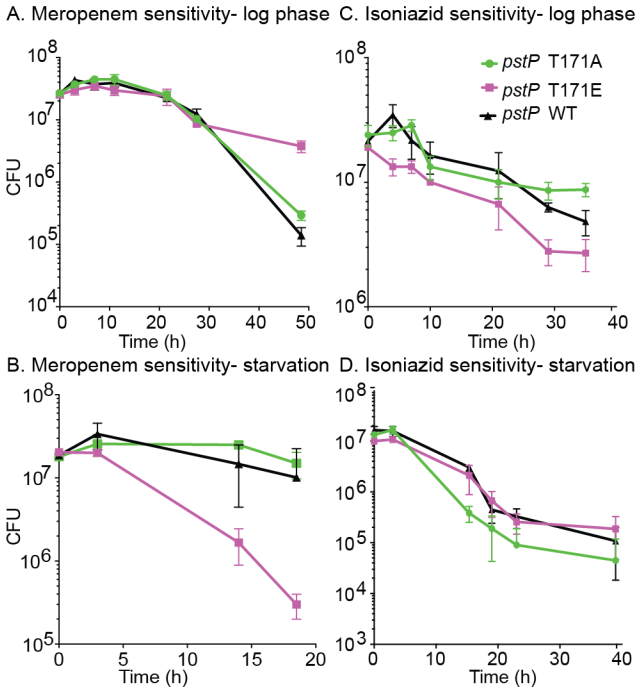

442

443 **FIG 4 Phospho-site T171 of PstP plays a role in antibiotic sensitivity.**

444 (A) Survival curve of *pstP* allele strains (WT, T17A and T171E) grown in 7H9 treated with 8ug/ml

445 of Meropenem.

446 (B) Survival curve of isogenic *pstP* allele strains starved in HdB (no Glycerol, 0.05% Tween) for

447 five and a half hours and then treated with 45ug/ml of Meropenem.

448 (C) Survival curve of *pstP* allele strains (WT, T17A and T171E) grown in 7H9 treated with

449 10ug/ml of Isoniazid.

450 (D) Survival curve of isogenic *pstP* allele strains starved in HdB (no Glycerol, 0.05% Tween) for

451 five and a half hours and then treated with 90ug/ml of Isoniazid.

452

453 The slower growth of the *pstP*$_{Msmeg}$ T171E strain in log. phase may account for
454 the greater tolerance in that condition. The apparent failure of the *pstP*$_{Msmeg}$
455 T171E strain to downregulate PG synthesis (Fig. 3D) likely makes it more
456 sensitive to PG inhibitors in starvation.
457 Next, we treated our wild-type and *pstP*$_{Msmeg}$ T171 mutant strains with isoniazid,
458 which targets InhA in the FAS-II pathway of mycolic acid synthesis (74). In log.
459 phase, we see that the *pstP*$_{Msmeg}$ T171E strain is more susceptible to isoniazid
460 than the *pstP*$_{Msmeg}$ T171A and the wild-type strains (Fig. 4C). Phosphorylation
461 inhibits the activity of InhA (30, 32). Our model is that, PstP might be the
462 phosphatase of InhA and the T171E phospho-form may dephosphorylate InhA~P
463 more slowly than the unphosphorylated form in log. phase. Thus the pool of
464 active InhA may be decreased in the T171E strain and the cells are sensitized to
465 further InhA inhibition by isoniazid. Another possibility is that PstP$_{Msmeg}$ T171E
466 likely cannot properly regulate its activity against the FAS-II enzymes, and the
467 misregulation of the pathway increases sensitivity to pathway inhibitors. We don't
468 see significant differences in isoniazid sensitivity between the strains in starvation
469 (Fig. 4D), which corroborates the observation that there is no difference in DMN-
470 Tre staining either in starvation (Fig. 3E). Thus, it seems that phosphorylation on
471 T171 affects PstP's activity against FAS-II enzymes in log. phase, but not
472 starvation.
473
474
475

476 **PstP$_{Mtb}$ dephosphorylates CwlM$_{Mtb}$**

477

478 Only a few endogenous substrates of PstP have been reported: some STPKs
479 including PknA and PknB, (39, 49, 51, 52), KasA and KasB (27, 49, 51), and
480 EmbR (50). The STPK PknB phosphorylates CwlM, which is a regulator of PG
481 biosynthesis (26). The phosphoform of CwlM interacts with and activates MurA
482 (26), the first enzyme in PG precursor synthesis pathway (34). CwlM is rapidly
483 dephosphorylated in transition to starvation in *Msmeg* (26), and becomes hyper-
484 phosphorylated when PstP is depleted in *Msmeg* (36).

485

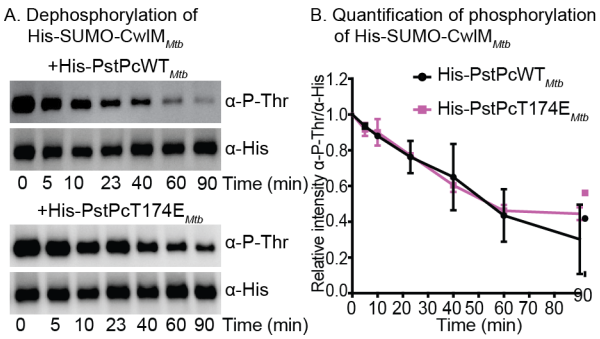

486

487 **FIG 5 PstP$_{Mtb}$ dephosphorylates CwlM$_{Mtb.}$**

488 (A) α-P-Thr and α-His Western blots of *in vitro* phosphatase reactions with His-PstP$_c$WT$_{Mtb}$ (top
489 panel) and His-PstP$_c$T174E$_{Mtb}$ (bottom panel) and phosphorylated His-SUMO-CwlM$_{Mtb}$. Assay was
490 performed at least twice with two individually purified batches of each phosphatase, one set of
491 images is shown here.

492 (B) Quantification of relative intensities of α-P-Thr and α-His signal on Western blot using ImageJ.
493 The graph was plotted with relative intensities of α-P-Thr/relative intensities of α-His from assay
494 performed with different preparations of His-PstP$_c$WT$_{Mtb\ and}$ His-PstP$_c$T174E$_{Mtb.}$

495

496

497 To test whether PstP directly dephosphorylates CwlM, we performed an in *vitro*
498 biochemical assay with purified *Mtb* proteins. We purified His-MBP-PknB$_{Mtb}$, His-
499 SUMO-CwlM$_{Mtb}$ and the cytoplasmic region of PstPWT$_{Mtb}$ (His-PstP$_{c,}$WT$_{Mtb}$). We
500 phosphorylated His-SUMO-CwlM$_{Mtb}$ by His-MBP-PknB$_{Mtb}$, stopped the
501 phosphorylation reaction with Calf Intestinal Phosphatase, and then added His-
502 PstP$_{c}$WT$_{Mtb}$ to His-SUMO-CwlM$_{Mtb}$~P. We found that the phosphorylation signal
503 on His-SUMO-CwlM$_{Mtb}$ started decreasing within 5 minutes after addition of His-
504 PstP$_{c}$WT$_{Mtb}$ and kept decreasing over a period of 90 minutes (Fig. 5A, top panel).
505 This is direct biochemical evidence that CwlM$_{Mtb}$ is a substrate of PstP$_{Mtb.}$ These
506 data with *Mtb* proteins support our model that PstP regulates PG metabolism by
507 dephosphorylating CwlM.
508
509 **Phosphosite T174 of PstP$_{Mtb}$ does not affect rate of dephosphorylation of**
510 **CwlM$_{Mtb}$ *in vitro***
511
512 Our data in Fig. 3D suggest that phosphorylation on PstP$_{Msmeg}$ T171 impacts PG
513 metabolism in starvation, possibly by downregulating PstP's dephosphorylation
514 activity against CwlM~P. We wanted to see if phosphorylation on the
515 corresponding phosphosite T174 in PstP$_{Mtb}$ affected its activity in
516 dephosphorylating CwlM$_{Mtb}$ *in vitro*.
517
518 PstP can dephosphorylate itself (49), so the purified form is unphosphorylated.
519 We performed a phosphatase assay with His-PstP$_{c}$T174E$_{Mtb}$ and His-SUMO-

520 CwlM$_{Mtb}$ (Fig. 5A, bottom panel). We observed that the WT and T174
521 phosphomimimetic forms of PstP$_{Mtb}$ have similar rates of activity against His-
522 SUMO-CwlM$_{Mtb}$ *in vitro* (Fig. 5B).
523
524 **Discussion**
525
526 Previous studies on mycobacterial phospho-regulation suggest that PstP could
527 play a critical role in modulating cell wall metabolism in the transition between
528 growth and stasis (26, 27, 36, 49, 52, 53, 71, 75). In this work, we explored how
529 the phosphorylation of PstP contributes to this regulation. We report here that the
530 phospho-site T171 of PstP$_{Msmeg}$ impacts growth, cell wall metabolism and
531 antibiotic tolerance. We found that the PG master regulator CwlM$_{Mtb}$ is a
532 substrate of PstP$_{Mtb}$.
533 Our findings indicate that the phosphorylation on PstP affects PG metabolism in
534 stasis and the mycolic acid metabolism during growth.
535
536 PstP's phospho-site T171 helps regulate reductive cell division. The cell length of
537 *Msmeg* has been observed to decrease from ~5μm to ~1.5μm in certain carbon
538 starvation conditions (66). It is assumed that this is due to reductive cell division
539 (68, 76), wherein the relative activity of division increases compared to
540 elongation. We consider this an increase in division/elongation. In *Mtb*, cell length
541 increases in chronic infection through destabilization of FtsB (77); this involves
542 decreasing division/elongation activity. Thus, both *Msmeg* and *Mtb* change their

543 relative division and elongation activities depending on environment, leading to
544 changes in cell length. We understand very little about the factors that control this
545 regulation. In *E. coli* and *B. subtilis*, cell length is increased in nutrient rich
546 conditions through inhibition of the assembly of division factor FtsZ (78, 79).
547
548 How might PstP help regulate the division/elongation balance in mycobacteria?
549 In *Mtb*, FtsZ's GTPase activity and polymerization is inhibited by phosphorylation,
550 catalyzed by PknA (80). If PstP is the phosphatase for FtsZ, its activity should
551 promote division. In the transition to starvation, *Msmeg* increases
552 division/elongation, and we might expect that PstP would be even more active
553 against FtsZ, thus promoting division. Or, PstP could decrease elongation. RodA,
554 which is likely to be a elongative PG transglycosylase (81, 82) seems to be
555 activated by phosphorylation in *Mtb* (82). So, PstP could dephosphorylate RodA
556 to slow elongation, thus increasing division/elongation. Our data show that the
557 $PstP_{Msmeg}$ T171 phospho-mimetic strain fails to reductively divide (Fig. 2C) in
558 stasis. If PstP's putative activity against FtsZ or RodA is critical for this reductive
559 cell division, then phosphorylation on T171 may inhibit PstP's activity against
560 both FtsZ and RodA. PstP has not yet been shown to dephosphorylate FtsZ or
561 RodA, but it is known to dephosphorylate PknA (49), the kinase for FtsZ and
562 PknB the kinase for RodA (82).
563
564 PstP seem to control PG and mycolic acid metabolism differently in growth and
565 the transition to stasis. Our data suggest that PstP T171 mainly regulates PG in

566 the transition to stasis (Fig. 3D and F) while its role in mycolic acid metabolism
567 may be restricted to log. phase (Fig. 3B and C). PG is activated by
568 phosphorylation at several points along the biosynthesis pathway (26, 35, 82,
569 83). PknB likely serves as a master regulator and checkpoint in this pathway by
570 detecting periplasmic lipid II (84), and changing its phosphorylation of PG factors
571 in response. PstP may not be very active against these factors in log. phase,
572 which would explain why the mutations at T171 of PstP do not affect PG
573 metabolism in growth (Fig. 3A and C).
574
575 Synthesis of the various cell wall layers must be synchronized to maintain cell
576 wall integrity. We think that PknB is a big player in connecting PG and mycolic
577 acid metabolism during growth. If PG metabolism is slowed, PknB could sense
578 the accumulation of periplasmic lipid II (84) and signal to halt mycolic acid
579 biosynthesis by inactivating the FAS-II enzymes and the trehalose monomycolate
580 transporter MmpL3 (85) via phosphorylation (27-32, 85). Our data imply that PstP
581 helps balance the effects of these inhibitory phosphorylations to allow
582 coordinated growth in log. phase (Fig. 3B and C). Misphosphorylation of PstP
583 likely disrupts this coordination and seems to decrease mycolic acid metabolism.
584 It is likely that other regulatory systems such as transcriptional control by SigB,
585 Rel, SigE or MtrA (71, 86-89), (90) predominate over phosphorylation in
586 controlling mycolic acid synthesis in the transition to stasis (Fig. 3E and F).
587

588 The phosphorylation of PstP may govern its interaction with other proteins or
589 localization in order to control substrate specificity. Our data (Fig. 3D) show that
590 the $PstP_{Msmeg}$ T171 phosphomimetic strain fails to downregulate PG in starvation
591 *in vivo*. We expect that PstP's activity against the PG master regulator CwlM (Fig
592 5A, top panel) should be critical for this downregulation because it should de-
593 activate MurA, the first enzyme in PG precursor synthesis (26, 34). In view of the
594 *in vivo* data, we expected that the $PstP_{Msmeg}$ T174E phosphomimetic variant
595 would dephosphorylate CwlM more slowly *in vitro*, but we observed no difference
596 in dephosphorylation rate (Fig. 5B). Why does this phosphosite not affect PstP's
597 activity *in vitro*? The proximity of a phosphosite to the substrate binding site of an
598 enzyme may affect the catalytic activity directly (91) but T174 maps to the β-
599 sheet core (β8) in $PstP_{Mtb}$, which is distant from the active site (Fig. 1A) (48). *In*
600 *vivo*, it is possible that phosphorylation at this site may affect PstP's interaction
601 with other regulatory proteins (92) that could affect activity against different
602 substrates, or it could affect access to substrates via localization changes.
603 Nevertheless, the effect of this phospho-site on PstP's catalytic activity need to
604 be tested on more substrates in future studies.
605
606 We see that PstP regulates antibiotic tolerance in *Msmeg* in both growth and
607 stasis. Our staining experiments imply that PstP T171 influences mycolic acid
608 synthesis in growth (Fig. 3B and C) and PG synthesis in starvation (Fig. 3D and
609 F). Our tests of tolerance to killing by mycolic acid-targeting (Fig. 4C) and PG-
610 targeting (Fig. 4B) antibiotics corroborate the staining data. We propose that

611 PstP may be an Achilles' heel of *Mtb*. It is an essential enzyme, so inhibiting it
612 should kill growing *Mtb* directly. But, it is also a master regulator of antibiotic
613 tolerance under stress, so inhibiting PstP should misregulate the cell wall and
614 increase permeability to other antibiotics.
615
616 **Acknowledgment**
617
618 This work was supported by grant 1R15GM131317-01 from the National
619 Institutes of Health, and by startup funds from the University of Texas at
620 Arlington. We thank Kenan Murphy for the plasmids pDE54MCZD and pKM55
621 and Dirk Schnappinger for pDE43-MCS and RevTetR promoter plasmids used in
622 this study.
623
624
625
626
627
628
629
630
631
632
633
634
635

636 **References:**

637 1. **World Health Organization**. 2019. Global Tuberculosis Report 2019.

638 2. **Nguyen L**. 2016. Antibiotic resistance mechanisms in M.
639 tuberculosis: an update. Arch Toxicol **90**:1585–1604.

640 3. **Jarlier V**, **Nikaido H**. 1994. Mycobacterial cell wall: structure and role
641 in natural resistance to antibiotics. **123**:11–18.

642 4. **Seiler P**, **Ulrichs T**, **Bandermann S**, **Pradl L**, **Jörg S**, **Krenn V**,
643 **Morawietz L**, **Kaufmann SHE**, **Aichele P**. 2003. Cell-wall alterations
644 as an attribute of Mycobacterium tuberculosis in latent infection. J
645 Infect Dis **188**:1326–1331.

646 5. **Wallis RS**, **Patil S**, **Cheon SH**, **Edmonds K**, **Phillips M**, **Perkins MD**,
647 **Joloba M**, **Namale A**, **Johnson JL**, **Teixeira L**, **Dietze R**, **Siddiqi S**,
648 **Mugerwa RD**, **Eisenach K**, **Ellner JJ**. 1999. Drug tolerance in
649 Mycobacterium tuberculosis. Antimicrobial Agents and Chemotherapy
650 **43**:2600–2606.

651 6. **Bhamidi S**, **Shi L**, **Chatterjee D**, **Belisle JT**, **Crick DC**, **McNeil MR**.
652 2012. A bioanalytical method to determine the cell wall composition of
653 Mycobacterium tuberculosis grown in vivo. ANALYTICAL
654 BIOCHEMISTRY **421**:240–249.

655 7. **Cunningham AF**, **Spreadbury CL**. 1998. Mycobacterial stationary
656 phase induced by low oxygen tension: cell wall thickening and

657 localization of the 16-kilodalton alpha-crystallin homolog. J Bacteriol
658 **180**:801–808.

659 8. **Sarathy J**, **Dartois V**, **Dick T**, **Gengenbacher M**. 2013. Reduced
660 Drug Uptake in Phenotypically Resistant Nutrient-Starved
661 Nonreplicating Mycobacterium tuberculosis. Antimicrobial Agents and
662 Chemotherapy **57**:1648–1653.

663 9. **Minnikin DE**. 1991. Chemical principles in the organization of lipid
664 components in the mycobacterial cell envelope. Research in
665 Microbiologoy **142**:423–427.

666 10. **Kieser KJ**, **Rubin EJ**. 2014. How sisters grow apart: mycobacterial
667 growth and division. Nature Publishing Group 1–13.

668 11. **Marrakchi H**, **Lanéelle M-A**, **Daffé M**. 2014. Mycolic Acids:
669 Structures, Biosynthesis, and Beyond. Chemistry & Biology **21**:67–85.

670 12. **Hett EC**, **Rubin EJ**. 2008. Bacterial growth and cell division: a
671 mycobacterial perspective. Microbiol Mol Biol Rev **72**:126–56– table
672 of contents.

673 13. **Hoffmann C**, **Leis A**, **Niederweis M**, **Plitzko JM**, **Engelhardt H**.
674 2008. Disclosure of the mycobacterial outer membrane: cryo-electron
675 tomography and vitreous sections reveal the lipid bilayer structure.
676 Proc Natl Acad Sci USA **105**:3963–3967.

677 14. **Jarlier V**, **Nikaido H**. 1990. Permeability barrier to hydrophilic solutes
678 in Mycobacterium chelonei. J Bacteriol **172**:1418–1423.

679 15. **Echenique J**, **Kadioglu A**, **Romao S**, **Andrew PW**, **Trombe MC**.
680 2004. Protein Serine/Threonine Kinase StkP Positively Controls
681 Virulence and Competence in Streptococcus pneumoniae. Infection
682 and immunity **72**:2434–2437.

683 16. **Juris SJ**, **Rudolph AE**, **Huddler D**, **Orth K**, **Dixon JE**. 2000. A
684 distinctive role for the Yersinia protein kinase: actin binding, kinase
685 activation, and cytoskeleton disruption. Proceedings of the National
686 Academy of Sciences **97**:9431–9436.

687 17. **Galyov EE**, **Hakansson S**, **Forsberg A**, **Wolf-Watz H**. 1993. A
688 secreted protein kinase of Yersinia pseudotuberculosis is an
689 imdispensable virulence determinant 1–3.

690 18. **Wang J**, **Li C**, **Yang H**, **Mushegian A**, **Jin S**. 1998. A novel
691 serine/threonine protein kinase homologue of Pseudomonas
692 aeruginosa is specifically inducible within the host infection site and is
693 required for full virulence in neutropenic mice. J Bacteriol **180**:6764–
694 6768.

695 19. **Gee CL**, **Papavinasasundaram KG**, **Blair SR**, **Baer CE**, **Falick AM**,
696 **King DS**, **Griffin JE**, **Venghatakrishnan H**, **Zukauskas A**, **Wei JR**,
697 **Dhiman RK**, **Crick DC**, **Rubin EJ**, **Sassetti CM**, **Alber T**. 2012. A

698 Phosphorylated Pseudokinase Complex Controls Cell Wall Synthesis
699 in Mycobacteria. Science Signaling **5**:ra7–ra7.

700 20. **Cole ST**, **Brosch R**, **Parkhil J**, **Garnier T**. 1998. Deciphering the
701 biology of Mycobacterium tuberculosisfrom the complete genome
702 sequence 1–27.

703 21. **Bach H**, **Wong D**, **Av-Gay Y**. 2009. Mycobacterium tuberculosisPtkA
704 is a novel protein tyrosine kinase whose substrate is PtpA. Biochem J
705 **420**:155–162.

706 22. **Sassetti CM**, **Boyd D**, **Rubin EJ**. 2003. Genes required for
707 mycobacterial growth defined by high density mutagenesis 1–8.

708 23. **Kang CM**. 2005. The Mycobacterium tuberculosis serine/threonine
709 kinases PknA and PknB: substrate identification and regulation of cell
710 shape. Genes & Development **19**:1692–1704.

711 24. **Fernandez P**, **Saint-Joanis B**, **Barilone N**, **Jackson M**, **Gicquel B**,
712 **Cole ST**, **Alzari PM**. 2006. The Ser/Thr Protein Kinase PknB Is
713 Essential for Sustaining Mycobacterial Growth. J Bacteriol **188**:7778–
714 7784.

715 25. **Kusebauch U**, **Ortega C**, **Ollodart A**, **Rogers RS**, **Sherman DR**,
716 **Moritz RL**, **Grundner C**. 2014. Mycobacterium tuberculosis supports
717 protein tyrosine phosphorylation. Proceedings of the National
718 Academy of Sciences **111**:9265–9270.

719 26. **Boutte CC**, **Baer CE**, **Papavinasasundaram K**, **Liu W**, **Chase MR**,
720 **Meniche X**, **Fortune SM**, **Sassetti CM**, **Ioerger TR**, **Rubin EJ**, **Laub**
721 **M**. 2016. A cytoplasmic peptidoglycan amidase homologue controls
722 mycobacterial cell wall synthesis. eLife **5**:e14590.

723 27. **Molle V**, **Brown AK**, **Besra GS**, **Cozzone AJ**, **Kremer L**. 2006. The
724 Condensing Activities of the Mycobacterium tuberculosisType II Fatty
725 Acid Synthase Are Differentially Regulated by Phosphorylation.
726 Journal of Biological Chemistry **281**:30094–30103.

727 28. **Vilchèze C**, **Hards K**, **Berney M**, **Cook GM**, **Hartman T**. 2014.
728 Energetics of Respiration and Oxidative Phosphorylation in
729 Mycobacteria. Microbiology Spectrum **2**.

730 29. **Slama N**, **Leiba J**, **Eynard N**, **Daffé M**, **Kremer L**, **Quémard A**, **Molle**
731 **V**. 2011. Negative regulation by Ser/Thr phosphorylation of HadAB
732 and HadBC dehydratases from Mycobacterium tuberculosis type II
733 fatty acid synthase system. Biochemical and Biophysical Research
734 Communications **412**:401–406.

735 30. **Khan S**, **Nagarajan SN**, **Parikh A**, **Samantaray S**, **Singh A**, **Kumar**
736 **D**, **Roy RP**, **Bhatt A**, **Nandicoori VK**. 2010. Phosphorylation of
737 enoyl-acyl carrier protein reductase InhA impacts mycobacterial
738 growth and survival. Journal of Biological Chemistry **285**:37860–
739 37871.

740 31. **Veyron-Churlet R**, **Zanella-Cléon I**. 2010. Phosphorylation of the
741 Mycobacterium tuberculosis β-ketoacyl-acyl carrier protein reductase
742 MabA regulates mycolic acid biosynthesis. Journal of Biological ….

743 32. **Molle V**, **Gulten G**, **Vilchèze C**, **Veyron-Churlet R**, **Zanella-Cléon I**,
744 **Sacchettini JC**, **Jacobs WR Jr.**, **Kremer L**. 2010. Phosphorylation of
745 InhA inhibits mycolic acid biosynthesis and growth of Mycobacterium
746 tuberculosis. Mol Microbiol **78**:1591–1605.

747 33. **Vilchèze C**, **Molle V**, **Carrère-Kremer S**, **Leiba J**, **Mourey L**, **Shenai**
748 **S**, **Baronian G**, **Tufariello J**, **Hartman T**, **Veyron-Churlet R**, **Trivelli**
749 **X**, **Tiwari S**, **Weinrick B**, **Alland D**, **Guérardel Y**, **Jacobs WR**,
750 **Kremer L**. 2014. Phosphorylation of KasB Regulates Virulence and
751 Acid-Fastness in Mycobacterium tuberculosis. PLoS Pathog
752 **10**:e1004115.

753 34. **Marquardt JL**, **Siegele DA**, **Kolter R**, **Walsh CT**. 1992. Cloning and
754 sequencing of Escherichia coli murZ and purification of its product, a
755 UDP-N-acetylglucosamine enolpyruvyl transferase. J Bacteriol
756 **174**:5748–5752.

757 35. **Turapov O**, **Forti F**, **Kadhim B**, **Ghisotti D**, **Sassine J**, **Straatman-**
758 **Iwanowska A**, **Bottrill AR**, **Moynihan PJ**, **Wallis R**, **Barthe P**,
759 **Cohen-Gonsaud M**, **Ajuh P**, **Vollmer W**, **Mukamolova GV**. 2018.
760 Two Faces of CwlM, an Essential PknB Substrate, in Mycobacterium
761 tuberculosis. CellReports **25**:57–67.e5.

762 36. **Iswahyudi**, **Mukamolova GV**, **Straatman-Iwanowska AA**, **Allcock**
763 **N**, **Ajuh P**, **Turapov O**, **O'Hare HM**. 2019. Mycobacterial
764 phosphatase PstP regulates global serine threonine phosphorylation
765 and cell division. Scientific Reports **9**:8337.

766 37. **Sharma AK**, **Arora D**, **Singh LK**, **Gangwal A**, **Sajid A**, **Molle V**,
767 **Singh Y**, **Nandicoori VK**. 2016. Serine/Threonine Protein
768 Phosphatase PstP of Mycobacterium tuberculosis Is Necessary for
769 Accurate Cell Division and Survival of Pathogen. Journal of Biological
770 Chemistry **291**:24215–24230.

771 38. **DeJesus MA**, **Gerrick ER**, **Xu W**, **Park SW**, **Long JE**, **Boutte CC**,
772 **Rubin EJ**, **Schnappinger D**, **Ehrt S**, **Fortune SM**, **Sassetti CM**,
773 **Ioerger TR**. 2017. Comprehensive Essentiality Analysis of the
774 Mycobacterium tuberculosis Genome via Saturating Transposon
775 Mutagenesis. mBio **8**.

776 39. **Chopra P**, **Singh B**, **Singh R**, **Vohra R**, **Koul A**, **Meena LS**, **Koduri**
777 **H**, **Ghildiyal M**, **Deol P**, **Das TK**, **Tyagi AK**, **Singh Y**. 2003.
778 Phosphoprotein phosphatase of Mycobacterium tuberculosis
779 dephosphorylates serine–threonine kinases PknA and PknB.
780 Biochemical and Biophysical Research Communications **311**:112–
781 120.

782 40. **Barford D**. 1996. Molecular mechanisms of the protein
783 serine/threonine phosphatases. Trends Biochem Sci **21**:407–412.

784 41. **Cohen P**. 1989. The structure and regulation of protein
785 phosphatases. Annu Rev Biochem **58**:453–508.

786 42. **Mougous JD**, **Gifford CA**, **Ramsdell TL**, **Mekalanos JJ**. 2007.
787 Threonine phosphorylation post-translationally regulates protein
788 secretion in Pseudomonas aeruginosa. Nat Cell Biol **9**:797–803.

789 43. **Irmler A**, **Forchhammer K**. 2001. A PP2C-type phosphatase
790 dephosphorylates the PII signaling protein in the cyanobacterium
791 Synechocystis PCC 6803. Proceedings of the National Academy of
792 Sciences **98**:12978–12983.

793 44. **Vijay S**, **Mukkayyan N**, **Ajitkumar P**. 2014. Highly Deviated
794 Asymmetric Division in Very Low Proportion of Mycobacterial Mid-log
795 Phase Cells. Open Microbiol J **8**:40–50.

796 45. **Bradshaw N**, **Levdikov VM**, **Zimanyi CM**, **Elife RG**. 2017. A
797 widespread family of serine/threonine protein phosphatases shares a
798 common regulatory switch with proteasomal proteases.
799 cdnelifesciencesorg

800 .

801 46. **Lu G**, **Wang Y**. 2008. FUNCTIONAL DIVERSITY OF MAMMALIAN
802 TYPE 2C PROTEIN PHOSPHATASE ISOFORMS: NEW TALES
803 FROM AN OLD FAMILY. Clinical and Experimental Pharmacology
804 and Physiology **35**:107–112.

805 47. **Vijay K**, **Brody MS**, **Fredlund E**, **Price CW**. 2000. A PP2C
806 phosphatase containing a PAS domain is required to convey signals
807 of energy stress to the sigmaB transcription factor of Bacillus subtilis.
808 Mol Microbiol **35**:180–188.

809 48. **Pullen KE**, **Ng H-L**, **Sung P-Y**, **Good MC**, **Smith SM**, **Alber T**. 2004.
810 An Alternate Conformation and a Third Metal in PstP/Ppp, the M.
811 tuberculosis PP2C-Family Ser/Thr Protein Phosphatase. Structure
812 **12**:1947–1954.

813 49. **Sajid A**, **Arora G**, **Gupta M**, **Upadhyay S**, **Nandicoori VK**, **Singh Y**.
814 2011. Phosphorylation of Mycobacterium tuberculosis Ser/Thr
815 Phosphatase by PknA and PknB. PLoS ONE **6**:e17871–11.

816 50. **Sharma K**, **Gupta M**, **Krupa A**, **Srinivasan N**, **Singh Y**. 2006. EmbR,
817 a regulatory protein with ATPase activity, is a substrate of multiple
818 serine/threonine kinases and phosphatase in Mycobacterium
819 tuberculosis. FEBS J **273**:2711–2721.

820 51. **Durán R**, **Villarino A**, **Bellinzoni M**, **Wehenkel A**, **Fernandez P**,
821 **Boitel B**, **Cole ST**, **Alzari PM**, **Cerveñansky C**. 2005. Conserved
822 autophosphorylation pattern in activation loops and juxtamembrane
823 regions of Mycobacterium tuberculosis Ser/Thr protein kinases.
824 Biochemical and Biophysical Research Communications **333**:858–
825 867.

826 52. **Boitel B**, **Ortiz-Lombardía M**, **Durán R**, **Pompeo F**, **Cole ST**,
827 **Cerveñansky C**, **Alzari PM**. 2003. PknB kinase activity is regulated
828 by phosphorylation in two Thr residues and dephosphorylation by
829 PstP, the cognate phospho-Ser/Thr phosphatase, in Mycobacterium
830 tuberculosis. Mol Microbiol **49**:1493–1508.

831 53. **Dulberger CL**, **Rubin EJ**, **Boutte CC**. 2020. The mycobacterial cell
832 envelope - a moving target. Nature Publishing Group **18**:47–59.

833 54. **Hartmans S**, **De Bont JAM**. 1992. The genus *Mycobacterium*—
834 nonmedical, 2nd ed. Springer-Verlag New York Inc., New York, NY.

835 55. **Murphy KC**, **Papavinasasundaram K**, **Sassetti CM**. 2015.
836 Mycobacterial recombineering. Methods Mol Biol **1285**:177–199.

837 56. **Schnappinger D**, **O'Brien KM**, **Ehrt S**. 2015. Construction of
838 conditional knockdown mutants in mycobacteria. Methods Mol Biol
839 **1285**:151–175.

840 57. **Pashley CA**, **Parish T**. 2003. Efficient switching of
841 mycobacteriophage L5-based integrating plasmids in Mycobacterium
842 tuberculosis. FEMS Microbiology Letters **229**:211–215.

843 58. **Ducret A**, **Quardokus EM**, **Brun YV**. 2016. MicrobeJ, a tool for high
844 throughput bacterial cell detection and quantitative analysis. Nature
845 Microbiology **1**:671–7.

846 59. **Kieser KJ**, **Boutte CC**, **Kester JC**, **Baer CE**, **Barczak AK**, **Meniche**
847 **X**, **Chao MC**, **Rego EH**, **Sassetti CM**, **Fortune SM**, **Rubin EJ**. 2015.
848 Phosphorylation of the Peptidoglycan Synthase PonA1 Governs the
849 Rate of Polar Elongation in Mycobacteria. PLoS Pathog **11**:e1005010.

850 60. **Gupta M**, **Sajid A**, **Arora G**, **Tandon V**, **Singh Y**. 2009. Forkhead-
851 associated domain-containing protein Rv0019c and polyketide-
852 associated protein PapA5, from substrates of serine/threonine protein
853 kinase PknB to interacting proteins of Mycobacterium tuberculosis.
854 Journal of Biological Chemistry **284**:34723–34734.

855 61. **van Kessel JC**, **Hatfull GF**. 2008. Mycobacterial recombineering.
856 Methods Mol Biol **435**:203–215.

857 62. **Cottin V**, **Van Linden A**, **Riches DW**. 1999. Phosphorylation of tumor
858 necrosis factor receptor CD120a (p55) by p42(mapk/erk2) induces
859 changes in its subcellular localization. J Biol Chem **274**:32975–32987.

860 63. **Su J**, **Forchhammer K**. 2012. Determinants for substrate specificity
861 of the bacterial PP2C protein phosphatase tPphA from
862 Thermosynechococcus elongatus. FEBS J **280**:694–707.

863 64. **Greenstein AE**, **Grundner C**, **Echols N**, **Gay LM**, **Lombana TN**,
864 **Miecskowski CA**, **Pullen KE**, **Sung P-Y**, **Alber T**. 2006.
865 Structure/Function Studies of Ser/Thr and Tyr Protein
866 Phosphorylation in Mycobacterium tuberculosis. J Mol

867 Microbiol Biotechnol **9**:167–181.

868 65. **Schlicker C**, **Fokina O**, **Kloft N**, **Grüne T**, **Becker S**, **Sheldrick GM**,
869 **Forchhammer K**. 2008. Structural Analysis of the PP2C
870 Phosphatase tPphA from Thermosynechococcus elongatus: A
871 Flexible Flap Subdomain Controls Access to the Catalytic Site.
872 Journal of Molecular Biology **376**:570–581.

873 66. **Wu M-L**, **Gengenbacher M**, **Dick T**. 2016. Mild Nutrient Starvation
874 Triggers the Development of a Small-Cell Survival Morphotype in
875 Mycobacteria. Front Microbiol **7**:100.

876 67. **Kuru E**, **Hughes HV**, **Brown PJ**, **Hall E**, **Tekkam S**, **Cava F**, **de**
877 **Pedro MA**, **Brun YV**, **VanNieuwenhze MS**. 2012. In Situ Probing of
878 Newly Synthesized Peptidoglycan in Live Bacteria with Fluorescent
879 D-Amino Acids. Angew Chem Int Ed **51**:12519–12523.

880 68. **Baranowski C**, **Rego EH**, **Rubin EJ**. 2019. The Dream of a
881 Mycobacterium. Microbiology Spectrum **7**.

882 69. **Kamariza M**, **Shieh P**, **Ealand CS**, **Peters JS**, **Chu B**, **Rodriguez-**
883 **Rivera FP**, **Babu Sait MR**, **Treuren WV**, **Martinson N**, **Kalscheuer**
884 **R**, **Kana BD**, **Bertozzi CR**. 2018. Rapid detection of Mycobacterium
885 tuberculosis in sputum with a solvatochromic trehalose probe. Sci
886 Transl Med **10**.

887 70. **Deb C**, **Lee C-M**, **Dubey VS**, **Daniel J**, **Abomoelak B**, **Sirakova TD**,

888 **Pawar S**, **Rogers L**, **Kolattukudy PE**. 2009. A Novel In Vitro
889 Multiple-Stress Dormancy Model for Mycobacterium tuberculosis
890 Generates a Lipid-Loaded, Drug-Tolerant, Dormant Pathogen. PLoS
891 ONE **4**:e6077.

892 71. **Betts JC**, **Lukey PT**, **Robb LC**, **McAdam RA**, **Duncan K**. 2002.
893 Evaluation of a nutrient starvation model of Mycobacterium
894 tuberculosis persistence by gene and protein expression profiling. Mol
895 Microbiol **43**:717–731.

896 72. **Zhang Y**. 2003. Zhang 2004 1–21.

897 73. **Wayne LG**, **Hayes LG**. 1996. An In Vitro Model for Sequential Study
898 of Shiftdown of. Infection and immunity **64**:2062–2069.

899 74. **Marrakchi H**, **Lanéelle G**, **Quémard A**. 2000. InhA, a target of the
900 antituberculous drug isoniazid, is involved in a mycobacterial fatty
901 acid elongation system, FAS-II. Microbiology (Reading, Engl) **146 (Pt**
902 **2)**:289–296.

903 75. **Ortega C**, **Liao R**, **Anderson LN**, **Rustad T**, **Ollodart AR**, **Wright**
904 **AT**, **Sherman DR**, **Grundner C**. 2014. Mycobacterium tuberculosis
905 Ser/Thr Protein Kinase B Mediates an Oxygen-Dependent Replication
906 Switch. Plos Biol **12**:e1001746–11.

907 76. **Smeulders MJ**, **Keer J**, **Speight RA**, **Williams HD**. 1999. Adaptation
908 of Mycobacterium smegmatis to stationary phase. J Bacteriol

909 **181**:270–283.

910 77. **Wang R**, **Kreutzfeldt K**, **Botella H**, **Vaubourgeix J**, **Schnappinger**
911 **D**, **Ehrt S**. 2019. Persistent Mycobacterium tuberculosis infection in
912 mice requires PerM for successful cell division. eLife **8**.

913 78. **Weart RB**, **Lee AH**, **Chien A-C**, **Haeusser DP**, **Hill NS**, **Levin PA**.
914 2007. A Metabolic Sensor Governing Cell Size in Bacteria. Cell
915 **130**:335–347.

916 79. **Hill NS**, **Buske PJ**, **Shi Y**, **Levin PA**. 2013. A Moonlighting Enzyme
917 Links Escherichia coli Cell Size with Central Metabolism. PLoS Genet
918 **9**:e1003663.

919 80. **Thakur M**, **Chakraborti PK**. 2006. GTPase activity of mycobacterial
920 FtsZ is impaired due to its transphosphorylation by the eukaryotic-
921 type Ser/Thr kinase, PknA. J Biol Chem **281**:40107–40113.

922 81. **Meeske AJ**, **Riley EP**, **Robins WP**, **Uehara T**, **Mekelanos JJ**, **Kahne**
923 **D**, **Walker S**, **Kruse AC**, **Bernhardt TG**, **Rudner DZ**. 2016. SEDS
924 proteins are a widespread family of bacterial cell wall polymerases.
925 Nature 1–15.

926 82. **Arora D**, **Chawla Y**, **Malakar B**, **Singh A**, **Nandicoori VK**. 2018. The
927 transpeptidase PbpA and noncanonical transglycosylase RodA of
928 Mycobacterium tuberculosis play important roles in regulating
929 bacterial cell lengths. Journal of Biological Chemistry **293**:6497–6516.

930 83. **Kieser KJ**, **Baranowski C**, **Chao MC**, **Long JE**, **Sassetti CM**,
931 **Waldor MK**, **Sacchettini JC**, **Ioerger TR**, **Rubin EJ**. 2015.
932 Peptidoglycan synthesis in Mycobacterium tuberculosisis organized
933 into networks with varying drug susceptibility. Proceedings of the
934 National Academy of Sciences **112**:13087–13092.

935 84. **Kaur P**, **Rausch M**, **Malakar B**, **Watson U**, **Damle NP**, **Chawla Y**,
936 **Srinivasan S**, **Sharma K**, **Schneider T**, **Jhingan GD**, **Saini D**,
937 **Mohanty D**, **Grein F**, **Nandicoori VK**. 2019. LipidII interaction with
938 specific residues of Mycobacterium tuberculosis PknB
939 extracytoplasmic domain governs its optimal activation. Nature
940 Communications **10**:7470–17.

941 85. **Le N-H**, **Locard-Paulet M**, **Stella A**, **Tomas N**, **Molle V**, **Burlet-**
942 **Schiltz O**, **Daffé M**, **Marrakchi H**. 2020. The protein kinase PknB
943 negatively regulates biosynthesis and trafficking of mycolic acids in
944 mycobacteria. J Lipid Res.

945 86. **Lee KK**, **Jang CS**, **Yoon JY**, **Kim SY**, **Kim TH**, **Ryu KH**, **Kim W**.
946 2008. Abnormal cell division caused by inclusion bodies in E. coli;
947 increased resistance against external stress. Microbiological
948 Research **163**:394–402.

949 87. **Dahl JL**, **Kraus CN**, **Boshoff HIM**, **Doan B**, **Foley K**, **Avarbock D**,
950 **Kaplan G**, **Mizrahi V**, **Rubin H**, **Barry CE**. 2003. The role of RelMtb-
951 mediated adaptation to stationary phase in long-term persistence of

952 Mycobacterium tuberculosis in mice. Proceedings of the National
953 Academy of Sciences **100**:10026–10031.

954 88. **Carette X**, **Platig J**, **Young DC**, **Helmel M**, **Young AT**, **Wang Z**,
955 **Potluri L-P**, **Moody CS**, **Zeng J**, **Prisic S**, **Paulson JN**, **Muntel J**,
956 **Madduri AVR**, **Velarde J**, **Mayfield JA**, **Locher C**, **Wang T**,
957 **Quackenbush J**, **Rhee KY**, **Moody DB**, **Steen H**, **Husson RN**. 2018.
958 Multisystem Analysis of Mycobacterium tuberculosisReveals Kinase-
959 Dependent Remodeling of the Pathogen-Environment Interface. mBio
960 **9**:193–21.

961 89. **Lee J-H**, **Karakousis PC**, **Bishai WR**. 2008. Roles of SigB and SigF
962 in the Mycobacterium tuberculosis sigma factor network. J Bacteriol
963 **190**:699–707.

964 90. **Manganelli R**, **Voskuil MI**, **Schoolnik GK**, **Smith I**. 2001. The
965 Mycobacterium tuberculosis ECF sigma factor sigmaE: role in global
966 gene expression and survival in macrophages. Mol Microbiol **41**:423–
967 437.

968 91. **Veyron-Churlet R**, **Molle V**, **Taylor RC**, **Brown AK**, **Besra GS**,
969 **Zanella-Cléon I**, **Fütterer K**, **Kremer L**. 2009. The Mycobacterium
970 tuberculosisβ-Ketoacyl-Acyl Carrier Protein Synthase III Activity Is
971 Inhibited by Phosphorylation on a Single Threonine Residue. J Biol
972 Chem **284**:6414–6424.

973 92. **Lin K**, **Hwang PK**, **Fletterick RJ**. 1997. Distinct phosphorylation
974 signals converge at the catalytic center in glycogen phosphorylases.
975 Structure **5**:1511–1523.

976
977
978
979
980
981
982
983
984
985
986
987
988
989
990
991
992
993
994
995
996
997

998 Figure S1

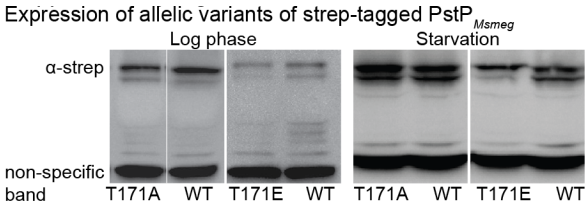

999

1000

1001 Figure S1: α-strep Western blots of allelic variants of strep-tagged PstP$_{Msmeg}$ in log (left

1002 panel) and starvation phase (right panel). A non-specific band at the bottom in all strains

1003 was seen in the blots.

1004

1005